

## Research article

# Multi-scale visual analysis of cycle characteristics in spatially-embedded graphs

Farhan Rasheed<sup>a,\*</sup>, Talha Bin Masood<sup>a</sup>, Tejas G. Murthy<sup>b</sup>, Vijay Natarajan<sup>c</sup>, Ingrid Hotz<sup>a</sup>

<sup>a</sup> Department of Science and Technology, Linköping University, Bredgatan 33, Norrköping, 60221, Sweden

<sup>b</sup> Department of Civil Engineering, Indian Institute of Science, Bangalore, 560012, India

<sup>c</sup> Department of Computer Science and Automation, Indian Institute of Science, Bangalore, 560012, India

## ARTICLE INFO

## Article history:

Received 24 May 2023

Accepted 27 June 2023

Available online 1 July 2023

## Keywords:

Visual data analysis

Planar graph

Force network

Granular materials

Persistence homology

Force loops

Computational geometry

## ABSTRACT

We present a visual analysis environment based on a multi-scale partitioning of a 2d domain into regions bounded by cycles in weighted planar embedded graphs. The work has been inspired by an application in granular materials research, where the question of scale plays a fundamental role in the analysis of material properties. We propose an efficient algorithm to extract the hierarchical cycle structure using persistent homology. The core of the algorithm is a filtration on a dual graph exploiting Alexander's duality. The resulting partitioning is the basis for the derivation of statistical properties that can be explored in a visual environment. We demonstrate the proposed pipeline on a few synthetic and one real-world dataset.

© 2023 The Authors. Published by Elsevier B.V. on behalf of Zhejiang University and Zhejiang University Press Co. Ltd. This is an open access article under the CC BY-NC-ND license (<http://creativecommons.org/licenses/by-nc-nd/4.0/>).

## 1. Introduction

In this paper, we present a visual analysis method for planar graphs embedded in a 2d spatial domain. It is based on a hierarchical partitioning of the underlying space into regions bounded by cycles in the graph serving as a basis for the aggregation of multi-level statistics of properties. The work has been motivated by a collaboration with scientists studying granular materials. These are dense materials composed of discrete particles, such as sand or grains, that interact through interparticle contact forces building force networks (Papadopoulos et al., 2018). One of the driving questions in this research is to derive macro-scale properties from the particle interactions at the micro-scale structure, e.g., by averaging some local measures over a representative volume element (RVE). However, the relationship between the micro- and macro-scale interactions is complex and there is neither clarity as to what good descriptive properties are nor the scales of RVEs (Shahin et al., 2022). For two-dimensional granular materials, (Cambou et al., 2016) introduced a “meso-scale” to bridge the gap between micro- and macro-scales. They proposed subdividing the domain into “meso-domains” defined by “loops” in the particle connectivity graph. The particles contained inside these loops, so-called “rattlers”, do not directly contribute to force propagations in the material. Generalizing the ideas from this work, our first goal was to build a framework for a multi-scale

decomposition of a 2d domain into areas bound by connectivity, or force-loops, serving as a basis for the aggregation of summary properties.

To address this problem, we formulate this task in a more general and data-centric way. If one interprets the force networks as two-dimensional, planar, weighted graphs embedded in a continuous, spatial domain, the loops can be defined as cycles in the graph. The multi-scale aspect can be achieved by considering a set of subgraphs restricted to edges with a weight greater than a given threshold. This is a well-known topological problem that can be addressed using persistent homology by applying filtration over the edge weights. However, most algorithmic implementations only keep track of the number of independent cycles without providing an explicit set of generators (a basis) of the cycle group. Because this set is not unique, various criteria for selecting an appropriate basis have been proposed, often employing a minimality criterion. In our case, the condition is that the generator set provides a space partition. For an efficient computation of the generators, we propose an algorithm that applies dual filtering based on Alexander's duality, exploiting the spatial embedding of the graph. For the resulting hierarchical partitioning of the domain, a series of structural and shape measures are aggregated across the spatial segments. An exploratory visualization environment links the results for interactive analysis, combining the representation of the partitions, the hierarchical tree, and statistical plots of the aggregated metrics. An overview of the pipeline is shown in Fig. 1. We demonstrate the method on

\* Corresponding author.

E-mail address: [farhan.rasheed@liu.se](mailto:farhan.rasheed@liu.se) (F. Rasheed).

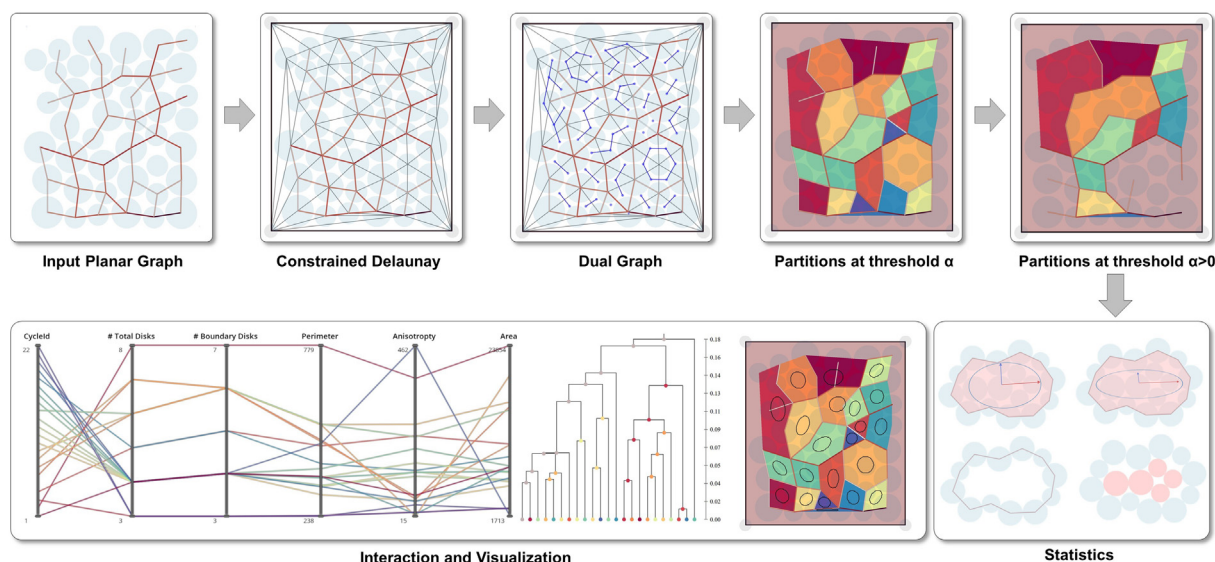


**Fig. 1.** Pipeline: The main steps in the computation of the hierarchical partitioning (Section 4) are illustrated in the first row. The method takes a weighted planar graph as input. From this graph with boundary edges added, a constrained Delaunay triangulation is computed. Filtration on the dual graph generates a hierarchical partition of the domain. For every hierarchy-level summary statistics are computed that visualized in an interactive environment combining abstract and spatial renderings.

several analytical datasets and one dataset from granular materials. While motivated by a specific application, the concept applies more generally to embedded planar graphs such as transport networks. Our contributions can be summarized as:

- Formulation of an application-specific problem as a topological problem for embedded graphs.
- Efficient algorithm to solve this problem introducing a dual filtration.
- Aggregation of statistical measures on multiple scales, and integration of the analysis in a visualization environment.

The paper is structured as follows, it starts with an overview of related work in Section 2, then summarizes the necessary background from graph theory and topology in Section 3. Section 4 describes the method and central algorithm, followed by explaining the shape and structure measures in Section 5 used in the visual analysis environment, Section 6. The paper ends with a result section, Section 7, and a conclusion, Section 8.

## 2. Related work

We begin this short review with articles from the motivational application and then refer to work that has used topological methods in similar applications.

*Scales in granular materials* – As giving a complete overview of the work in this field goes well beyond this article, we are confining ourselves here to articles that have motivated our work. An overview of the network analysis of particles and grains can be found in the review article (Papadopoulos et al., 2018). Scales in granular systems play an increasingly important role in many of these works. Camabou et al. introduced the concept of a meso-scale to connect the macro-mechanical behavior of granular materials with the micro-scale grain interaction (Cambou et al., 2016). The meso-scale is defined by elementary loops in the contact network of grains. An idea that was then taken in several publications. Yang and Qi have developed a loop detection pipeline for contact network images (Yang and Qi, 2021). The stability of contact loops in simulated packings has been studied by Smart and Ottino, who compute loops in the network using a breadth-first search algorithm (Smart and Ottino, 2008). Zhu et al.

investigated how macroscopic mechanical behavior can be linked to the evolution of loops on the meso-scale (Zhu et al., 2017). Shahin et al. presented a study that emphasized that there is a hierarchy in the length scales for different properties of granular solids (Shahin et al., 2022). Going beyond contact networks, the role of force networks was examined in Daniels (2017). To quantify the local organization of the grains and the anisotropy in the material a wide set of local measures have been introduced including scalar and tensor valued measures (Kuhn et al., 2015; Wan et al., 2005). We also use such tensors to aggregate material properties at different scales.

*Topological methods* used for the analysis of granular materials range from Morse theory-based methods for segmenting particles in CT images (Pandey et al., 2022) to characterizing the “shape of data” (Hiraoka, 2019). Persistent homology has also been used to quantify structural changes in networks (Hajij et al., 2018). In the context of granular materials, (Kramár et al., 2014b) define chain complexes for the analysis and comparison of 2D particle networks. This work was later extended to describe dynamic properties in these networks using persistence diagrams for comparison (Kondic et al., 2017; Kramár et al., 2014a). These works bear a certain resemblance to ours. However, their analysis is restricted to networks and does not consider properties in the embedding space.

*Cycles* generally play an important role in the analysis of graphs and networks, and there are many advanced methods for cycle extraction (Kavitha et al., 2009). However, due to the specific requirements on cycles in our application to create spatial partitioning, most of the methods cannot be applied directly.

## 3. Background

The method and algorithm presented in this work are based on fundamental concepts from graph theory and topology are briefly summarized below. Although the term *loop* is more commonly used to refer to cycles in force networks in the material science literature, we will use the term *cycle* following the terminology used in the topology literature in the rest of the paper.

### 3.1. Graph theory, definitions, and notations

A graph  $G$  is defined as a pair  $(V, E)$  of a set of vertices  $V$  and a set of edges  $E$  (Jungnickel, 2012). An edge  $e = (u, v) \in E$  is an unordered pair connecting its incident vertices, or endpoints  $u, v \in V$ . The degree of a vertex  $v$  is the number of edges incident on  $v$ . We restrict our discussion to simple graphs that can have at most one edge between a pair of vertices. A weighted graph has numerical weights assigned to its edges. That is, there is a scalar function defined on the set of edges,  $f : E \rightarrow \mathbb{R}$ .

A subgraph  $G' = (V', E')$  of  $G$  is a graph such that  $V' \subseteq V$  and  $E' \subseteq E$ . A cycle  $C$  is a subgraph such that each vertex in  $C$  has an even degree. The sum of two cycles  $C_i + C_j$  can be defined as a subgraph such that the set of edges is the symmetric difference of the edges in  $C_i$  and  $C_j$ . Note that the  $C_i + C_j$  is also a cycle. A circuit is a cycle that only has degree 2 nodes and forms a single connected component. A minimal set of cycles is called a cycle basis if all the cycles in the graph can be written as a sum of some of the cycles in the basis.

A spatial embedding of a graph in a plane maps each vertex to a point  $(x, y) \in \mathbb{R}^2$  while each edge is mapped to some curve connecting the locations of its endpoints. A graph is called planar if it has a spatial embedding such that none of the edges intersect. A planar straight-line graph is a spatial embedding of a planar graph such that edges are mapped to straight line segments connecting the vertices. It is known that such an embedding always exists for any planar graph. We assume our input graph is a spatially embedded straight-line graph with positive edge weights.

### 3.2. Topology background

Topology deals with the study of properties of shapes that are invariant under continuous deformations. Homotopy and homology provide algebraic tools to compare topological spaces (Hatcher, 2002). We focus our discussion on simplicial homology that provides a combinatorial computationally-friendly framework for representing topological spaces and computing their invariants.

#### 3.2.1. Simplicial homology

In simplicial homology, any topological space is represented using a combinatorial structure called a simplicial complex which is composed of small building blocks called simplices (Edelsbrunner, 2006). A general  $d$ -dimensional simplex is the convex hull of  $d + 1$  affinely independent points. Restricting to 2D, the three types of simplices of interest are vertices, edges, and triangles, in increasing dimension from 0 to 2 respectively. A simplex  $\tau$  is a face of another simplex  $\sigma$  if its constituent vertices are a non-empty proper subset of the vertices of  $\sigma$ . A simplicial complex  $K$  is then defined as a finite collection of simplices such that two conditions are satisfied: (i) if  $\sigma \in K$ , then all of its faces  $\tau$  are also part of  $K$ ; and, (ii) any two simplices  $\sigma_1$  and  $\sigma_2$  either share a common face or their intersection is empty. A subcomplex of  $K$  is a simplicial complex  $L \subseteq K$ .

Homology provides a robust framework for defining and computing topological invariants for a simplicial complex using homology groups. To define homology groups, we first need to define a few key concepts such as chains, boundaries, and cycles. A  $d$ -chain is a subset of the  $d$ -simplices in  $K$ . Two  $d$ -chains can be added by taking their symmetric difference. The set of  $d$ -chains together with this addition operation forms an algebraic group called chain group denoted as  $C_d$ . The boundary of a  $(d + 1)$ -simplex is the set of its  $d$  dimensional faces. A  $d$ -boundary of a  $(d + 1)$ -chain is obtained by taking the sum of boundaries of the simplices in the  $(d + 1)$ -chain. The set of  $d$ -boundaries form a subgroup

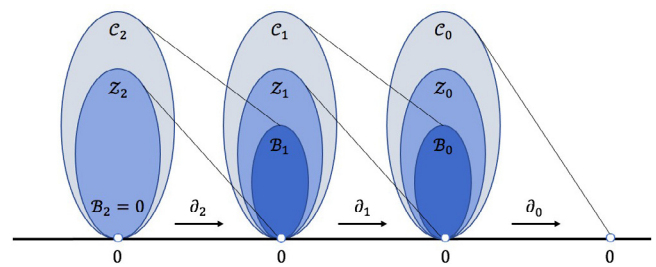


Fig. 2. Chain complex for 2D simplicial complex.

called boundary group  $B_d$  within  $C_d$ . A  $d$ -chain with zero boundary is called a  $d$ -cycle. The set of  $d$ -cycles form a subgroup called cycle group  $Z_d$  of  $C_d$ . One of the fundamental theorems in homology shows that any  $d$ -boundary is also a  $d$ -cycle. Therefore, we have the following nesting relationship within the aforementioned algebraic groups:  $B_d \subseteq Z_d \subseteq C_d$ .

The boundary homomorphism  $\partial_d : C_d \rightarrow C_{d-1}$  maps a  $d$ -chain to the sum of the boundaries of simplices in the  $d$ -chain. In other words,  $\partial_d$  is crucial in providing a connection between these group structures across the dimensions. Fig. 2 illustrates the relevant nesting of groups in various dimensions for a 2D simplicial complex and how they are connected by boundary homomorphism  $\partial_d$ , this structure is also called the chain complex. The  $d$ th homology group  $\mathcal{H}_d$  is defined as the quotient group  $Z_d/B_d$ . The rank of  $\mathcal{H}_d$  is also called the  $d$ th Betti number,  $\beta_d$  of  $K$ . An intuitive way to understand Betti numbers is  $\beta_d$  counts the number of  $d$ -dimensional holes in the simplicial complex. In low dimensions,  $\beta_0$  is equal to the number of connected components,  $\beta_1$  corresponds to the number of an independent set of one-dimensional cycles, while  $\beta_2$  captures the number of 2D cycles or voids in the complex. The Betti numbers of a simplicial complex are its topological invariants and can be used, for example, for determining if two shapes are topologically similar. If the sequence of Betti numbers of two spaces is the same, then they are also called homologous to each other.

#### 3.2.2. Persistent homology

Persistent homology studies the evolution of homology groups as simplices are removed or added based on some parameter, generating a filtration (Edelsbrunner and Harer, 2008). A filtration on  $K$  is a finite sequence of nested subcomplexes  $K_0 \subseteq K_1 \subseteq \dots \subseteq K_m = K$ , where each  $K_i$  is a subcomplex of  $K$ . For each  $i$ , we can compute the  $d$ th homology group  $\mathcal{H}_d(K_i)$ . This gives us a sequence of nested homology groups  $\mathcal{H}_d(K_0) \subseteq \mathcal{H}_d(K_1) \subseteq \dots \subseteq \mathcal{H}_d(K_m)$ . In practice, the filtration is usually defined by assigning scalar values  $f : K \rightarrow \mathbb{R}$  to the simplices in  $K$ , such that  $K_\alpha = \{\sigma \in K \text{ and } f(\sigma) > \alpha\}$  with the requirement that the scalar value of a simplex  $\sigma$  is less than the scalar values of all of its faces  $\tau$ . Varying the parameter  $\alpha$  provides the subcomplexes in the filtration.

A filtration of  $K$  can also be seen as building the complex by adding one simplex at a time in the decreasing order of scalar values. It then can be observed that the addition of a  $d$ -simplex to the simplicial complex either creates a new  $d$ -cycle or it destroys an existing  $(d - 1)$ -cycle, and therefore it affects the homology groups  $\mathcal{H}_d$  or  $\mathcal{H}_{d-1}$ . The lifetime of any  $d$ -cycle can be tracked from its birth due to the insertion of some  $d$ -simplex  $\sigma_i$  over the whole filtration during which it either dies due to the addition of a  $(d + 1)$ -simplex  $\sigma_j$  providing a persistence pair  $(\sigma_i, \sigma_j)$ , or it can survive till the end in which case it forms an essential cycle of  $K$ . The set of persistence pairs is often recorded and represented in the form of a scatter plot called persistence diagram or as a set of bars called persistence barcodes.

### 3.3. A view of graphs through the lens of topology

Any general graph represents a topological space and can be studied using the ideas from topology and homology. In particular, a spatially embedded straight-line graph can be viewed as a one-dimensional simplicial complex, where the graph vertices are its 0-simplices and the set of edges form its 1-simplices. The graph-theoretic definition of a cycle, i.e. a graph with even degree nodes, corresponds to the definition of 1-cycles in homology. The homology group  $\mathcal{H}_1$  for a graph is then isomorphic to the cycle group  $\mathcal{Z}_1$  as  $\mathcal{B}_1 = 0$  since there are no 2-simplices in a graph.

For weighted graphs the edge weights provide a natural way to define filtration. After adding all the vertices, the edges can be added either in descending (or ascending) order of their edge weights to yield a filtration of the graph. A subgraph or a subcomplex  $G_\alpha$  is obtained by restricting to edges with weight greater than a given parameter value  $\alpha$ . The concise and robust summary of the evolution of 1-cycles provided by persistent homology tools like persistence diagrams can be used for analysis and comparison of weighted graphs.

### 3.4. Constrained Delaunay triangulation

For real-world data, geometric shapes are usually represented as a set of points in a plane or 3D space. The Delaunay triangulation, a concept from computational geometry (Aurenhammer et al., 2013), triangulates such a point set into non-overlapping triangles generating a simplicial complex (Edelsbrunner, 2006).

The constrained Delaunay triangulation (CDT) is a special case of Delaunay triangulation, which enforces certain edges or segments to be part of the triangulation. The resulting triangulation should be as close to a Delaunay triangulation as possible while still satisfying the constraints.

## 4. Computation of the hierarchical partitioning

In the following, we describe our algorithm for the generation of a multi-scale decomposition of a 2d domain into areas bound by cycles of a weighted planar straight-line graph. The core of the algorithm is a *dual filtration* of the embedding space, making use of Alexander's duality. The result is a spatial partitioning and a set of generators forming a basis of the cycle group. An overview of the main steps is shown in the first row of Fig. 1.

### 4.1. Alexander's duality

We build our algorithm on one of the key results in homology called Alexander's duality. We reproduce the statement as given in Hatcher (2002, Corollary 3.45).

**Theorem 1.** *If  $K$  is a compact, locally contractible, non-empty, proper subspace of  $n$  dimensional sphere  $S^n$ , then  $\tilde{\mathcal{H}}_d(S^n - K)$  is isomorphic to  $\tilde{\mathcal{H}}_{n-d-1}(K)$  for all  $d$ .*

Explaining all the intricacies and details of the theorem above is beyond the scope of this paper. So, we will only explain the relevant consequences of this theorem in the context of 2D simplicial homology. Let  $S^2$  be a simplicial complex topologically equivalent to a 2D sphere and let  $K$  be a subcomplex embedded in it. Then, the theorem states that there is a relationship between the homology groups of  $K$  and its complement  $S^2 - K$ . In fact, the following pairs of reduced homology groups: (i)  $\tilde{\mathcal{H}}_0(S^2 - K)$  and  $\tilde{\mathcal{H}}_1(K)$ , and (ii)  $\tilde{\mathcal{H}}_1(S^2 - K)$  and  $\tilde{\mathcal{H}}_0(K)$ , are isomorphic. The reduced homology groups are closely related to the homology groups defined earlier in Section 3.2. For  $d > 0$ , the reduced homology groups are the same as normal homology groups, i.e.,  $\tilde{\mathcal{H}}_d = \mathcal{H}_d$ . However, for any non-empty complex, the rank of 0th reduced homology group  $\tilde{\mathcal{H}}_0$  is 1 smaller than the rank of  $\mathcal{H}_0$ .

### 4.2. Dual graph definition

To reiterate, the input to our pipeline is a weighted planar straight line graph,  $G = (V, E)$ . This graph can have vertices with no incident edges. First, we compute the constrained Delaunay triangulation  $D$  for the vertices  $V$  which ensures that edges  $E$  are part of  $D$ . Both  $G$  and  $D$  can be considered as simplicial complexes. Furthermore,  $D$  is topologically homologous to a 2D disk. We can convert  $D$  to  $S^2$  (a 2D sphere) by adding an extra dummy point and connecting this point to the convex hull of  $D$  with some dummy edges and triangles. With this modification to  $D$ , we can use Alexander's duality to compute the cycles in  $G$  in a different way. Instead of extracting the generators of  $\mathcal{H}_1(G)$  which provides the cycle bases of the graph  $G$ , we compute the generators of  $\mathcal{H}_0(D - G)$  which is simply the connected components of  $D - G$ . As explained earlier, the number of connected components in  $D - G$  will be one greater than the number of 1-cycles in  $G$ .

However, the set of simplices  $D - G$  does not form a simplicial complex, as it contains triangles whose boundary edges are part of  $G$  and therefore not present in  $D - G$ . We remedy this issue by instead considering the *dual graph*  $\hat{G} = (\hat{V}, \hat{E})$  of  $D - G$ . The vertex set  $\hat{V}$  corresponds to the triangles in  $D - G$  while the edges  $\hat{E}$  are the edges in  $D$  that are not part of  $G$ . Now,  $\hat{G}$  is a simplicial complex such that  $\mathcal{H}_0(D - G)$  is isomorphic to  $\mathcal{H}_0(\hat{G})$  or in other words, both  $\hat{G}$  and  $D - G$  has the same number of connected components. Each connected component in  $\hat{G}$  corresponds to a set of connected triangles that defines a region in  $D$  whose boundary edges form a cycle, which is part of the  $G$ . Thereby, considering all connected components in  $\hat{G}$  partitions  $D$  into regions enclosed by cycles in  $G$ .

### 4.3. Filtration of $G$ and $\hat{G}$

The next step is to formulate the filtration at first over  $G$  and then its dual inverse filtration over  $\hat{G}$ .

To obtain a valid filtration of  $G$ , we need to extend the edge weights of  $G$  consistently to all the simplices in  $G$  and  $D$ . Therefore, let  $\omega$  be the maximum weight of an edge in  $G$ . All the vertices in  $D$  are then assigned a weight of  $\omega + \epsilon$  where  $\epsilon$  is a negligibly small positive number and the edges  $e \in D - G$  are assigned a weight of 0. Similarly, all the triangles in  $D$  are assigned the minimum weight, i.e. 0. Now, given a value  $\alpha$ , we can restrict  $G$  to a subcomplex  $G_\alpha := \{e \in G \mid w(e) > \alpha\}$ , containing edges with weight greater than  $\alpha$ . Note that  $G_\alpha$  is a valid simplicial complex as it will contain all the vertices in  $D$  considering they are assigned the maximum weight. As the parameter  $\alpha$  is decreased from  $\omega + \epsilon$  to 0,  $G_\alpha$  becomes larger, while simultaneously  $D - G_\alpha$  and therefore its dual graph  $\hat{G}_\alpha$  reduces in size. If we look at the parameter  $\alpha$  increasing from the value 0 to  $\omega + \epsilon$ , we find that we obtain a filtration for the dual graph  $\hat{G}_\alpha$ . In this dual setting, the filtration refers to the evolution of connected components in  $\hat{G}$  as the value of the parameter  $\alpha$  varies from 0 to  $\omega + \epsilon$ . The result of this filtration is a merge tree representing the evolution of the components, the spatial partitioning, and a set of cycle generators.

*Some algorithmic notes:* As we are not only interested in the merge events when increasing the value of  $\alpha$  but also the components and their boundaries we also keep track of the regions themselves and save their merge hierarchy. Starting with  $\alpha = 0$ , we compute the set of all connected components in  $\hat{G}_0$ , which correspond to all regions enclosed by cycles in  $G_0$ . We then select  $\alpha_1$  as the lowest edge weight in  $G$ . This entails removing edges with a weight less than or equal to  $\alpha_1$  in  $G_0$ . As a result,  $D - G_{\alpha_1}$  has more edges than  $D - G_{\alpha_0}$ , leading to the presence of edges in  $\hat{G}_{\alpha_1}$  that are not part of  $\hat{G}_{\alpha_0}$ . We then determine whether these edges

combine two or more disjoint components in  $\widehat{G}_{\alpha_0}$  (being at the boundary of two regions). If this is the case, then we label it as a merge event and store the connected components as a level in the hierarchy at  $\alpha_1$  otherwise we move to the next  $\alpha$  value. We then continue with increasing values of  $\alpha$  until  $\omega + \varepsilon$  to capture the entire evolution of partitioning. Thus, the evolution of connected components in  $\widehat{G}_\alpha$  as the value of  $\alpha$  changes can be computed efficiently using the union-find data structure, and the resulting hierarchy can be saved as a tree. The complexity of the algorithm is dominated by two operations, the Delaunay computation, and the union-find data structure. In our examples, the computation is interactive.

#### 4.4. Boundary treatment

Our input graph is a planar graph embedded in a finite 2-dimensional space. The first step of computing the constrained Delaunay triangulation, which is homologous to a disk. We, however, need a space equivalent to 2D sphere to apply Alexander's duality. As discussed before, we can do that by introducing a dummy vertex and connecting it to the convex hull. In our implementation, we chose to enclose the graph vertices with a box slightly bigger than the bounding box of the vertices. This is accomplished by adding four dummy vertices at the boundary and the four boundary edges are assigned the highest weight. Once the boundary is added, the partitioning of the entire domain includes an extra cycle corresponding to the boundary, which can be removed to obtain the cycles in the original graph. This extra cycle also helps in elegantly taking care of the one extra connected component in  $D - G$  compared to the number of 1-cycles in the  $G$  according to Alexander's duality.

### 5. Statistical property aggregation

In this section, we propose an exemplary set of local measures that enable quantitative analysis of the hierarchical partitioning and graph cycles. Most of the measures have been motivated by the application in granular materials, adapting common measures including scalar and tensorial entities.

*Scalar measures* – Scalar measures include network characteristics, such as average node degrees or edge weights, as well as spatial measures such as the enclosed area, or the perimeter of cycles. In the context of granular materials, the count of particles along the cycles or the number of enclosed particles is also of interest. We offer an aggregation over the spatial segments, all nodes enclosed by the cycle, or alternatively over the cycle boundary. Given the information that is readily available through our methods, all these values can be directly derived. The area can be obtained by summing the areas of the triangles within the cycles, while the lengths of boundary edges can be added together to determine the perimeter.

*Fabric tensor* – Fabric generally refers to directional characteristics of the microstructure of materials, e.g. in granular material. The fabric tensor quantifies such characteristics in a tensorial form. For granular materials different tensors summarizing different structural orientations represented by some vector  $n_i$  have been proposed, e.g. particle orientations, inter-particle contact normal directions, or the orientations of void shapes (Fu and Dafalias, 2015). A fabric tensor  $F$  is generally defined as

$$F = \frac{1}{N} \sum_{i=1}^N \omega_i n_i \otimes n_i$$

where  $n_i$  is the normalized direction and  $\omega_i$  some weight. The sum iterates over a volume element or its boundary. From these tensors, diverse anisotropy measures of the structure can be derived.

#### Algorithm 1: Compute cycle hierarchy for a spatially embedded weighted network

---

**Input** :  $G(V, E, w)$ ,  $w : E \rightarrow \mathbb{R}^+$   
**Output**:  $T$ , Tree encoding multi-scale cycle hierarchy

- 1  $\omega \leftarrow \max w(e)_{e \in E}$ ;
- 2 Determine the bounding box of  $V$   
 $(x_{min}, y_{min}), (x_{max}, y_{max})$ ;
- 3 Insert four dummy vertices to  $V$ :  
 $v_{00} = (x_{min} - \delta, y_{min} - \delta)$   
 $v_{01} = (x_{min} - \delta, y_{min} + \delta)$   
 $v_{10} = (x_{min} + \delta, y_{min} - \delta)$   
 $v_{11} = (x_{min} + \delta, y_{min} + \delta)$ ;
- 4 Insert boundary edges in  $E$  with weight  $\omega + \varepsilon$ :  
 $e_l = (v_{00}, v_{01})$   
 $e_r = (v_{10}, v_{11})$   
 $e_b = (v_{00}, v_{10})$   
 $e_t = (v_{01}, v_{11})$ ;
- 5  $D \leftarrow \text{ConstrainedDelaunay}(V, E)$ ;
- 6  $\forall \langle v_i, v_j \rangle \in D$ , with  
 $w'(\langle v_i, v_j \rangle) := \begin{cases} w(\langle v_i, v_j \rangle), & \text{if } \langle v_i, v_j \rangle \in G; \\ 0, & \text{otherwise} \end{cases}$ ;
- 7 Construct dual graph  $\widehat{G}_0 = (\widehat{V}, \widehat{E}_0)$   
 $\forall \Delta_i \in D$  insert a vertex  $v_{\Delta_i}$  in  $\widehat{V}$   
 $\forall$  edges  $e_i \in D$  with  $w(e_i) = 0$  insert a dual edge in  $\widehat{E}_0$  connecting the two incident triangles on  $e_i$
- 8 Use Union-Find datastructure  $UF$  to find the set of connected components  $C_0$  in  $\widehat{G}_0$
- 9 Insert leaf nodes corresponding to each component  $c_i$  in  $C_0$  in  $T$  and assign these leaf nodes a 0 weight
- 10 Initialize component to tree node index array  $M_{CT}$  with component  $M_{CT}[c_i] = n_i$
- 11 Sort  $E$  such that  $w_k < w_{k+1}$ ;
- 12 **foreach**  $e \in E$  **do**
- 13     Let  $e$  be incident on triangles  $\Delta_i$  and  $\Delta_j$ ;
- 14      $c_k \leftarrow \text{Find}(UF, v_{\Delta_i})$ ;
- 15      $c_l \leftarrow \text{Find}(UF, v_{\Delta_j})$ ;
- 16     **if**  $c_k \neq c_l$  **then**
- 17         Union( $UF, c_k, c_l$ );
- 18         Insert a node  $n_{kl}$  in  $T$  with children  $M_{CT}[c_k]$  and  $M_{CT}[c_l]$ ;
- 19         Assign weight  $w(e)$  to  $n_{kl}$ ;
- 20         Update  $M_{CT}[c_k] = M_{CT}[c_l] = n_{kl}$
- 21     **end**
- 22 **end**

---

We define two types of fabric tensors: loop tensor ( $S_L$ ) to quantify the shape of extracted cycles, similar to the one proposed in Cambou et al. (2016), and the force tensor ( $S_F$ ) taking the forces (weights) on the edges into account. For both tensors, we iterate over the edges within a cycle. The mathematical expression for both tensors is provided below:

$$S_L = \sum_{k=1}^N (\mathbf{p}_i^k - \mathbf{p}_j^k) \otimes (\widehat{\mathbf{p}_i^k - \mathbf{p}_j^k})$$

$$S_F = \sum_{k=1}^N w^k (\mathbf{p}_i^k - \mathbf{p}_j^k) \otimes (\widehat{\mathbf{p}_i^k - \mathbf{p}_j^k})$$

where  $(\widehat{\mathbf{p}_i^k - \mathbf{p}_j^k}) = \frac{(\mathbf{p}_i^k - \mathbf{p}_j^k)}{|\mathbf{p}_i^k - \mathbf{p}_j^k|}$ ,  $\mathbf{p}_i^k$  is the spatial coordinates of vertex  $i$  of edge  $k$ , while  $w^k$  is the weight of edge  $k$ .  $N$  represents the total number of edges forming the cycle. Fig. 3 illustrates an example

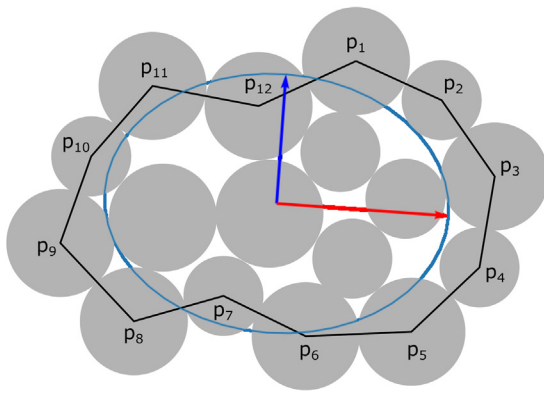


**Fig. 3.** Example of a cycle generated by particles ( $p_i$ ) in a granular material. The cycle is overlaid by the loop tensor along with the major and minor eigenvectors.

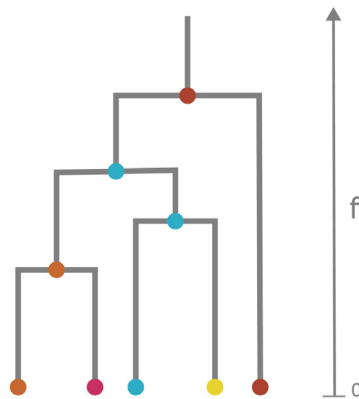


**Fig. 4.** A tree representation of the hierarchical evolution of regions enclosed by cycles as the filtration value increases. The leaves in the figure represent the cycles at a filtration value of zero, and the colors corresponds to the index of cycle. As the filtration value is increased, the cycles merge and eventually form a single component covering the whole domain. At merge, the cycle with highest perimeter retains its color while the other cycle dies. This representation is equivalent to a merge tree but for cycles.

of a cycle enclosed by force network edges in a granular system together with the its loop tensor.

**Anisotropy** – Anisotropy measures or quantifies the “directionality” of structures. One can find a large variety of explicit definitions of anisotropy for tensorial quantities in the literature. They are all based on the eigenvalues of the respective tensor using different normalizations. We define anisotropy as the absolute difference between the two eigenvalues which is inspired by the definition of shear stress in continuum mechanics

$$\text{anisotropy} = \Delta\lambda = |\lambda_1 - \lambda_2|$$

where  $\lambda_i$  are the eigenvalues.

### 6. Exploration and visualization

This section describes visualization components that facilitate the exploratory analysis of partitions in planar networks. The interactive rendering of cycle-enclosed regions is linked with a *parallel coordinates plot* displaying the cycle statistics. In addition, we provide a tree structure to convey the complete multi-scale summary of partitions. Overall, the resulting visualization components provide a powerful framework for exploring and analyzing partitioning within complex planar graphs. The proposed interactive visualization environment is implemented as a prototype in Inwiwo (Jönsson et al., 2019).

**Partitions visualization** – We provide the rendering of partitions overlaid by input planar graph along with the possibility of interactively changing the filtration value. Each partitioned region is assigned a unique color, while the edges in the planar graph are color-coded based on their weight. The colors of the regions are maintained throughout the filtration process; if two regions merge, the resulting region take on the color of the larger region. Further, we provide the possibility to overlay each region with the ellipse computed from the fabric tensors to directly visualize the orientation of the underlying region.

In the example of analyzing force networks in granular materials, the partitions are further overlaid on the granular system to visually evaluate the arrangement of disks within each region.

**Cycle statistics** – We present a parallel coordinates plot as a visual component to explore the characteristics of different regions in the partitioning. The properties of these regions, as described in Section 5, are represented as different coordinates in the plot. The parallel coordinates plot is linked with the rendering of partitions, such that each line in the plot corresponds to a unique region and gets the same color as its counterpart in the rendering. This feature facilitates easy comparison and selection of regions. The parallel coordinates plot also serves as an interface for filtering for specific regions in partitioning at some filtration value. Additionally, we provide brushing and linking capabilities, allowing users to highlight corresponding loops in the rendering by selecting lines in the parallel coordinates plot.

In addition to the visualization component that works on a single filtration level at a time, we present a tree-based visualization that provides an overview of the evolution of regions under varying filtration levels Fig. 4. The visualization enables tracking of regions’ appearance and merging at different filtration values. The leaf nodes of the tree represent the total number of cycles in the system at zero filtration. The inner nodes indicate the filtration values at which two regions merge. The height of the tree is scaled by the minimum and maximum filtration values, such that the y-coordinate of each node represents the actual filtration value.

When two cycles merge, one cycle dies, and we retain the cycle with the highest perimeter. The colors used in the system rendering correspond to the colors in the visualization. The proposed visualization technique provides an effective means for filtering or selecting force thresholds to study interesting structures.

## 7. Experimental results

In this section, we demonstrate our method in four different scenarios: (1) a simple graph with different embeddings, two synthetic datasets with varying edge weights in a dense graph, (2) examining its behavior modulating the edge weights by a concentric oscillating scalar field, (3) then defining the edge weights by a vector field with varying strength, and (4) finally applying our method to real-world data.

### 7.1. Simple graph

We first demonstrate our method using a simple weighted graph with different embeddings. Fig. 5 displays the input graphs, their constrained Delaunay triangulation, and their corresponding three hierarchical partitions. As the filtration threshold increases, the number of connected components decreases from two to zero for both graphs. As expected the result provides in both cases a hierarchical partitioning of the domain, with one component for  $w \geq 2$ , 2 components for  $w = 1$ , and three components for  $w = 0$ . However, the enclosing cycles are different for the two embeddings. As shown in Fig. 5 (second row at  $w = 0$ ), the shape

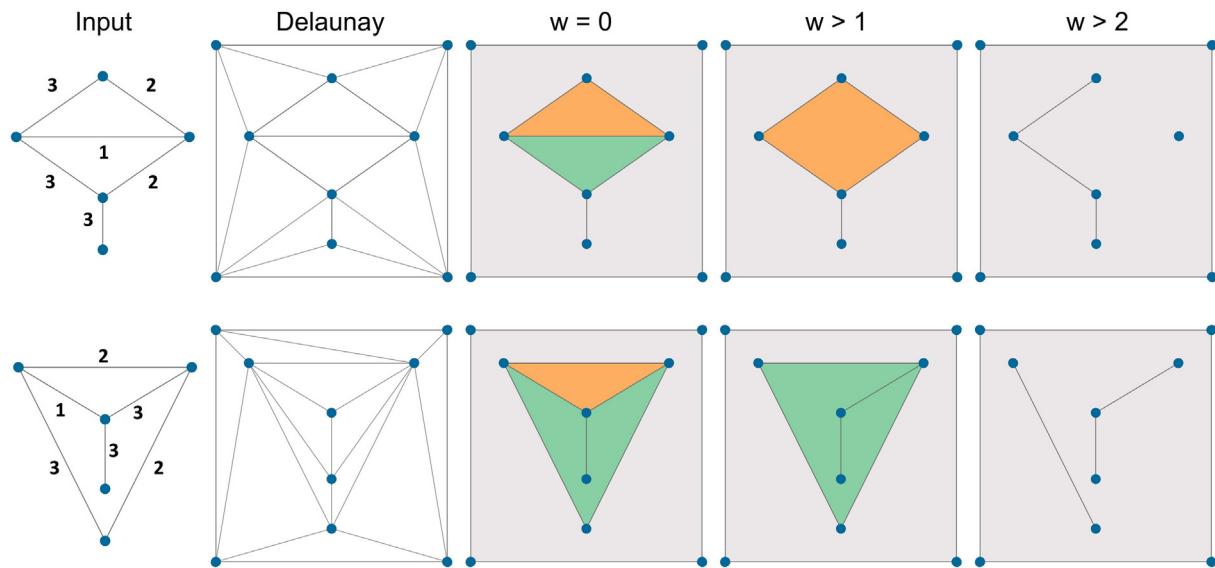


**Fig. 5.** Example of two simple graph datasets, followed by their Delaunay and hierarchy levels (left to right). Importantly, The partitions colored green in the second row at  $w = 0$  exhibit a non-convex shape, where its boundary is not a minimal generator.

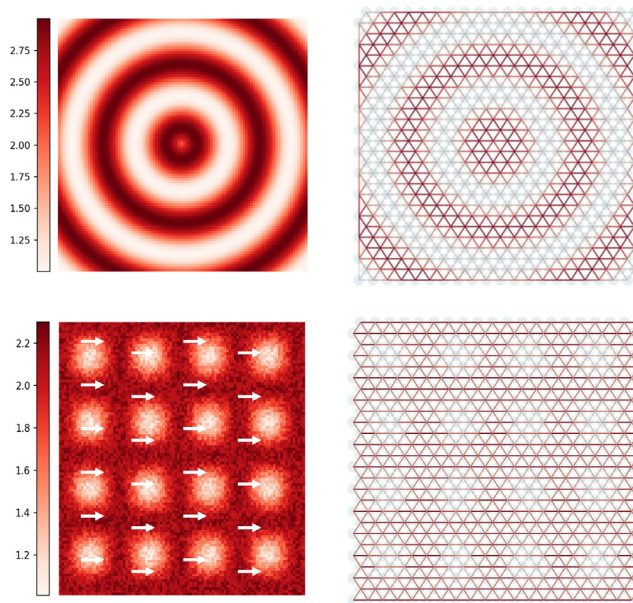


**Fig. 6.** Regular mesh (right) with edges sampled from the respective functions (left).

of the green partition is non-convex, which means its boundary does not represent the minimal cycles for this partition, which is frequently the criterion to define optimal cycle generators. The minimal generators would not provide a partitioning of the domain in non-overlapping regions.

### 7.2. Scalar field modulated edge weights

We designed this dataset in a way that we will obtain nested cycles during the filtration. The basic structure of the graph is a regular triangulation of a hexagonal mesh. The edge weights are generated by sampling a sinusoidal concentric using the following equation:

$$w(u, v) = f\left(\frac{u_x + v_x}{2}, \frac{u_y + v_y}{2}\right)$$

where  $f(x, y) := 2 + \sin(\sqrt{x^2 + y^2})$ . Fig. 6 (top row) shows the scalar function and the resulting regular mesh.

Fig. 7 shows the results at four filtration levels. At the small filtration level Fig. 7 (left), we obtained cycles including a lot of small “triangular” cycles consisting of three edges. Together they form a ring-like structure that encloses a large homogeneous ring component (light green) the boundary cycle of this component consists of two disconnected parts. As the filtration level increases, triangles with relatively less weight (triangles at the boundary of the ring) start to disappear, and a new cycle (blue) emerges from the center, as expected since it is sampled from a sinusoidal field with small values at the center.

### 7.3. Vector field modulated edge weights

We generate a dataset that is closer to our application. Here, we used an underlying vector field to modulate the edge weights. Similar to the previous example with the nested cycles, we use a regular mesh as the domain. The edge weights are now sampled from a vector field oriented in the  $x$ -direction scaled by a scalar function shown in Fig. 6 bottom row, the  $y$ -direction of the vectors is equal to zero. The edge weights result from a projection of this vector field onto the edges.

We show the resulting partitions at three different filtration levels for this mesh type Fig. 8. Due to the nature of edge weights, the horizontal edges exhibit comparatively higher weights compared to others. At low filtration levels, the patterns of the underlying vector field’s magnitude are still clearly visible. On increasing the scale, however, the directional edge weights become more dominant, resulting in rectangle-like partitions. Consequently, these partitions lead to anisotropic fabric tensors, which we visualize through the overlay of ellipses encompassing the direction. The evolution of the statistical measures during the filtration is shown in Fig. 9 (right). It clearly emphasizes the increase of anisotropy with the increasing filtration value.

### 7.4. Photoelastic disks dataset

Our last dataset is a result of an experiment with photoelastic disks, made of a material that changes color and intensity when subjected to mechanical stress. These materials are often used to study stress and force propagation in granular materials. By

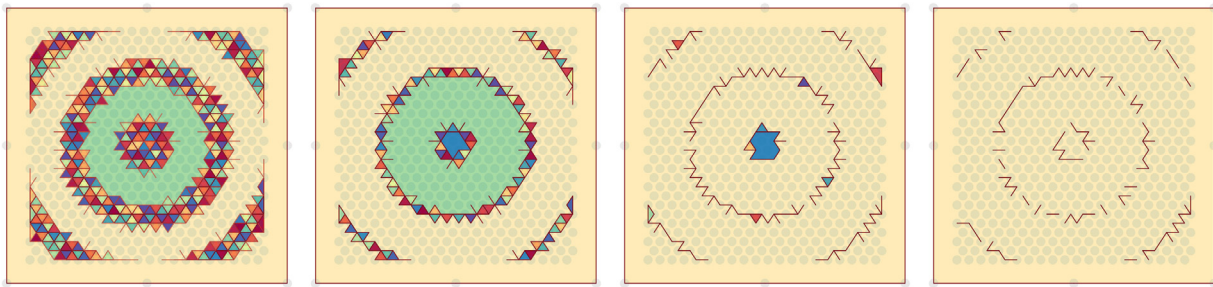


**Fig. 7.** Results from synthetic datasets generated on the regular mesh at four filtration levels. This example shows that our method can correctly deal with nested cycles in the graph.

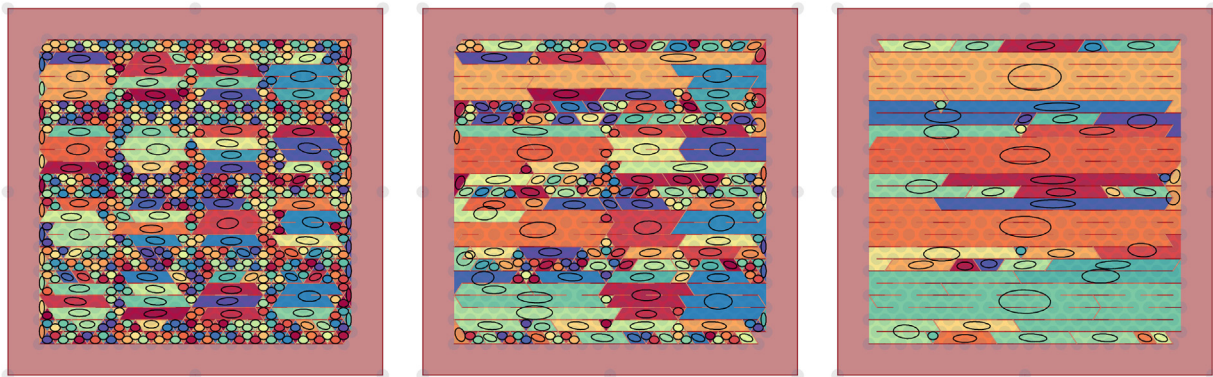


**Fig. 8.** Synthetic datasets generated on the regular mesh at three filtration levels. This example highlights the correct extraction of cycles aligning with the underlying vector field used for the generation of the edge weights. The fabric tensor represented as ellipses are overlaid on partitions.

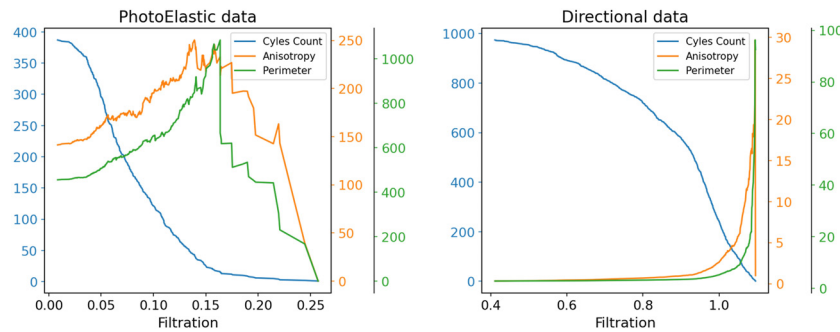


**Fig. 9.** Aggregation of cycle characteristics, anisotropy, perimeter along with cycle count as filtration varies.

analyzing the changes in the polarization of light passing through the photoelastic material, researchers can infer the force network within the granular material. The resulting force network is a perfect real-world example of planar graphs. Therefore, researchers are interested in gaining insights into the organization and force propagation within the granular material and studying its dynamics in response to external stresses. The concept of meso-scale based on particle contact cycles has been developed in the context of such experiments.

We obtained the dataset from collaborating domain experts which they generate by conducting experiments using photoelastic disks under different loading conditions. We apply our pipeline to the extracted force network for one loading condition and present the results in Fig. 10. The evolution of the statistical measures during the filtration is shown in Fig. 9 (left). It shows a peak in anisotropy at an intermediate filtration level.

### 8. Discussion and conclusion

In this paper, we have presented a novel approach to generate hierarchical sets of cycles in weighted spatially embedded graphs

using topological filtration. In contrast to previous approaches the proposed algorithm simultaneously extracts the cycle hierarchy, a set of cycle generators, and a spatial partitioning that serve as a basis for multi-scale analysis. The proposed algorithm is motivated by a collaboration with granular material scientists, however, solves a much more general problem. In the current version, we define our original filtration on the graph, a one-dimensional simplicial complex. As a positive consequence, we obtain uniquely defined cycle generators, however, this could also lead to a large set of cycles consisting only of three edges at a low filtration level. An extension of our algorithm excluding such cycles would require a slight adaptation of the selection of the set of cycle generators. In the long run, we consider extending the basic concept to generate hierarchical partitioning in three dimensions investigating hierarchical void structures.

We have demonstrated the method in a few synthetically designed examples to verify its performance and properties. We also applied the method to a dataset from the motivating application, however, the visual analysis has not yet been fully explored and utilized by our collaboration partners. Our environment provides

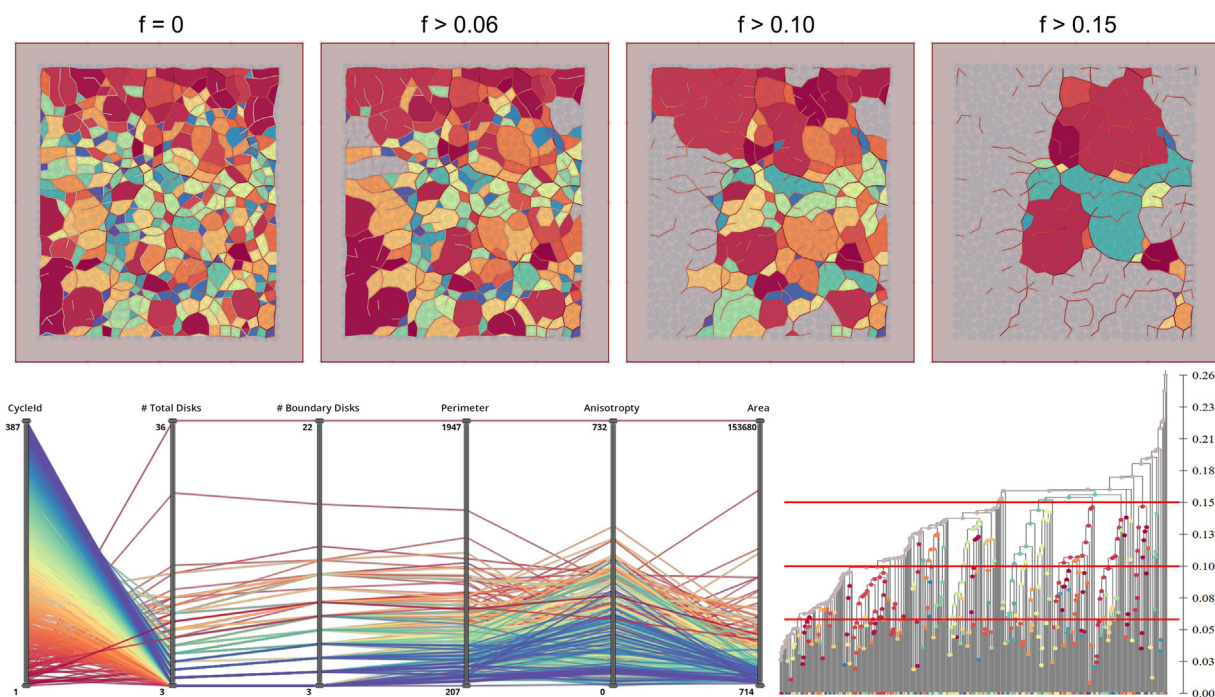


**Fig. 10.** Application to photoelastic data: System partitioning based on cycles in force network at four filtration levels (top). Each region gets its own color, while the network edges are colored according to their weight. Visualization of statistical measures in parallel coordinates plot for a filtration value and selection of desired cycles (bottom left). A hierarchical summary is provided by a tree (bottom right) with three hierarchy levels highlighted using red horizontal lines. The corresponding partitioning of these three levels is shown in the top row. The colors in every visualization component are consistent.

now a solid basis to go deeper into the application. One obvious next step is to evaluate the already implemented statistical measures and extend them with novel ideas from our partners. However, we also expect that there will be other conceptual adaptations necessary for the final use to explore granular materials.

### CRediT authorship contribution statement

**Farhan Rasheed:** Conceptualization, Methodology, Software, Writing – original draft, Visualization. **Talha Bin Masood:** Conceptualization, Methodology, Writing – review & editing. **Tejas G. Murthy:** Conceptualization, Data curation, Writing – review & editing. **Vijay Natarajan:** Conceptualization, Methodology, Writing – review & editing. **Ingrid Hotz:** Conceptualization, Methodology, Writing – review & editing, Supervision.

### Declaration of competing interest

The authors declare that they have no known competing financial interests or personal relationships that could have appeared to influence the work reported in this paper.

### Acknowledgments

This work was supported by the Wallenberg AI, Autonomous Systems and Software Program (WASP) funded by the Knut and Alice Wallenberg Foundation, the SeRC (Swedish e-Science Research Center) and the ELLIIT environment for strategic research in Sweden, the Swedish Research Council (VR) grant 2019–05487 and an Indo-Swedish joint network project: DST/INT/SWD/VR/P-02/2019 VR grant 2018–07085.

### Ethical approval

This study does not contain any studies with human or animal subjects performed by any of the authors.

### References

- Aurenhammer, F., Klein, R., Lee, D., 2013. *Voronoi Diagrams and Delaunay Triangulations*. World Scientific.
- Cambou, B., Magoaric, H., Nguyen, N.-S., 2016. 2 - definition of a meso-scale for granular materials. In: Cambou, B., Magoaric, H., Nguyen, N.-S. (Eds.), *Granular Materials At Meso-Scale*. Elsevier, pp. 25–48. <http://dx.doi.org/10.1016/B978-1-78548-065-2.50002-8>.
- Daniels, K.E., 2017. The role of force networks in granular materials. In: *EPJ Web of Conferences*. EDP Sciences, p. 01006.
- Edelsbrunner, H., 2006. *Geometry and Topology for Mesh Generation*, second ed. Cambridge Monographs on Applied and Computational Mathematics.
- Edelsbrunner, H., Harer, J., 2008. *Persistent homology – a survey*. In: Goodman, J.E., Pach, J., Pollack, R. (Eds.), *Surveys on Discrete and Computational Geometry: Twenty Years Later*, Vol. 458. AMS Bookstore, pp. 257–282.
- Fu, P., Dafalias, Y.F., 2015. Relationship between void- and contact normal-based fabric tensors for 2D idealized granular materials. *Int. J. Solids Struct.* 63, 68–81.
- Hajji, M., Wang, B., Scheidegger, C., Rosen, P., 2018. Visual detection of structural changes in time-varying graphs using persistent homology. In: *IEEE Pacific Visualization Symposium (PacificVis)*.
- Hatcher, A., 2002. *Algebraic Topology*. Cambridge University Press.
- Hiraoka, Y., 2019. Topological data analysis on materials science. Invited talk.
- Jönsson, D., Steneteg, P., Sundén, E., Englund, R., Kottravell, S., Falk, M., Ynnerman, A., Hotz, I., Ropinski, T., 2019. Inviwo - a visualization system with usage abstraction levels. *IEEE Trans. Vis. Comput. Graphics* 26 (11), 3241–3254. <http://dx.doi.org/10.1109/TVCG.2019.2920639>.
- Jungnickel, D., 2012. *Graphs, Networks and Algorithms*, fourth ed. In: *(Algorithms and Computation in Mathematics)*, Springer.
- Kavitha, T., Liebchen, C., Mehlhorn, K., Michail, D., Rizzi, R., Ueckerdt, T., Zweig, K.A., 2009. Cycle bases in graphs characterization, algorithms, complexity, and applications. *Comp. Sci. Rev.* 3, 199–243.
- Kondic, L., Kramár, M., Kovalčinová, L., Mischaikow, K., 2017. Evolution of force networks in dense granular matter close to jamming. In: *EPJ Web of Conferences*, Vol. 140. EDP Sciences, p. 15014.
- Kramár, M., Goulet, A., Kondic, L., Mischaikow, K., 2014a. Evolution of force networks in dense particulate media. *Phys. Rev. E* 90 (5), 052203.
- Kramár, M., Goulet, A., Kondic, L., Mischaikow, K., 2014b. Quantifying force networks in particulate systems. *Physica D* 283, 37–55.
- Kuhn, M.R., Sun, W., Wang, Q., 2015. Stress-induced anisotropy in granular materials: fabric, stiffness, and permeability. *Acta Geotech.*
- Pandey, K., Masood, T.B., Singh, S., Hotz, I., Natarajan, V., Murthy, T., 2022. Morse theory-based segmentation and fabric quantification of granular materials. *Granul. Matter* 24 (1).

- Papadopoulos, L., Porter, M.A., Daniels, K.E., Bassett, D.S., 2018. Review: Network analysis of particles and grains. *J. Complex Netw.* 6, 485–565.
- Shahin, G., Herbold, E.B., Hall, S.A., Hurley, R.C., 2022. Quantifying the hierarchy of structural and mechanical length scales in granular systems. *Extreme Mech. Lett.* 51.
- Smart, A.G., Ottino, J.M., 2008. Evolving loop structure in gradually tilted two-dimensional granular packings. *Phys. Rev. E* 77 (4), 041307.
- Wan, R., Guo, P., Al-Mamlun, M., 2005. Behaviour of granular materials in relation to their fabric dependencies. *Soils Found.* 45 (2), 77–86.
- Yang, J., Qi, Q., 2021. Study on meso-structure evolution in granular matters based on the contact loop recognition and determination technique. *Materials* 14 (21), 6542.
- Zhu, H., Veylon, G., Nicot, F., Darve, F., 2017. On the mechanics of meso-scale structures in two-dimensional granular materials. *Eur. J. Environ. Civ. Eng.* 21 (7–8), 912–935.